

Spatio-temporal Ca^{2+} dynamics of moth olfactory projection neurones

Mikael A. Carlsson,¹ Philipp Knüsel,² Paul F. M. J. Verschure² and Bill S. Hansson¹

¹Division of Chemical Ecology, Department of Crop Science, Swedish University of Agricultural Sciences, PO Box 44, SE-230 53 Alnarp, Sweden

²Institute of Neuroinformatics, ETH-Universität Zürich, Zürich, Switzerland

Keywords: coding, olfaction, optical imaging, projection neurones, *Spodoptera littoralis*

Abstract

We studied the Ca^{2+} dynamics of odour-evoked glomerular patterns in the antennal lobe of the moth *Spodoptera littoralis* using optical imaging. Here we selectively stained a large population of antennal lobe output neurones, projection neurones, by retrograde filling with FURA-dextran from the inner antennocerebral tract in the protocerebrum. Different plant-associated odorants evoked distributed patterns of activated glomeruli that were odour dependent and repeatable. These patterns were, however, dynamic during the period of odour exposure. Temporal responses differed across glomeruli and were stimulus dependent. Next we examined how the correlations between patterns evoked by different odorants changed with time. Initially, responses to structurally similar compounds were highly correlated, whereas responses to structurally different compounds differed. Within the period of odour exposure (1 s) we found a significant reduction in similarity of responses evoked by different odours, irrespective of initial similarity, whereas trial-to-trial correlations remained high. Our results suggested an ability for coarse classification at the initial encounter with an odour source. With time, however, the discrimination ability increases and structurally similar odours can be distinguished.

Introduction

Olfactory information might be encoded in the spatial distribution of neuronal activity, its temporal structure or a combination of both. A spatial encoding mechanism has been proposed in both the vertebrate olfactory bulb and the antennal lobe (AL) in insects (e.g. Johnson *et al.*, 1998; Galizia *et al.*, 1999; Kauer & White, 2001). In addition, information about odour identity and abundance is also carried in temporal patterns of coherently spiking neurones (Wehr & Laurent, 1996; Lei *et al.*, 2004) and in the slow temporal patterns in individual neurones (Laurent *et al.*, 1996). The concepts of temporal and spatial coding do not necessarily have to be in conflict, they could simply be two sides of the same coin (Laurent *et al.*, 2001; Laurent, 2002). Synchronous activity seems to be required for behavioural fine odour discrimination (Stopfer *et al.*, 1997) but abolishing coherent activity leaves the animal with an ability to discriminate dissimilar odours. The slow temporal patterns, on the other hand, may not be a code *per se* but rather a mechanism to optimize the spatio-temporal code over time (Laurent, 2002). In the moth *Manduca sexta* and in the locust it was recently demonstrated that classification of odour identity and abundance based on temporal patterns of coherent activity in AL neurones improved during the course of their presentation (Stopfer *et al.*, 2003; Daly *et al.*, 2004). Similar results were obtained from activity patterns across a population of responding mitral cells in the zebrafish (Friedrich & Laurent, 2001, 2004). Through selective staining of projection neurones (PNs) with a Ca^{2+} -sensitive dye, Sachse & Galizia (2002) recorded odour-dependent spatial activity patterns in the honeybee. In addition, Sachse & Galizia (2002)

observed that the activity patterns were not static during the stimulation period. Using a similar technique, we here specifically study these slow dynamic properties of PNs in the moth olfactory system.

In the insect AL, olfactory receptor neurones (ORNs) expressing the same type of olfactory receptors converge on the same glomerulus (Gao *et al.*, 2000; Vosshall *et al.*, 2000). Within a glomerulus, the ORNs synapse with the PNs. In addition, several morphological types of local interneurones (Anton & Homberg, 1999) connect ORNs with PNs and also make reciprocal synapses with PNs and feedback connections with ORNs. A major part of the local interneurones are immunoreactive to GABA (e.g. Tolbert & Hildebrand, 1981) and may thus act in an inhibitory fashion on target cells.

In earlier optical imaging studies in the moth *Spodoptera littoralis* we demonstrated that odour-evoked patterns of glomerular input activity were dependent on the stimulus identity and abundance and conserved across individuals (Carlsson *et al.*, 2002; Carlsson & Hansson, 2003; Meijerink *et al.*, 2003). Here we selectively stain and record changes in intracellular Ca^{2+} concentration in a large population of PNs with a moderately high temporal resolution. We addressed the questions of how different plant-related odorants were spatio-temporally represented among the PNs and the implication which this organization has on odour classification.

Materials and methods

Preparation of animals

Male *S. littoralis* were used 2–4 days post-emergence. The animals had been reared for several generations on a potato-based diet (Hinks

Correspondence: Dr Mikael A. Carlsson, as above.

E-mail: mikael.carlsson@vv.slu.se

Received 17 December 2004, revised 19 May 2005, accepted 25 May 2005

& Byers, 1976). The pupae were separated according to sex and kept in plastic boxes at 70% relative humidity, 23 °C and on a 16/8-h light/dark cycle. Adult moths were supplied with water *ad libitum* until the start of the experiment.

Animals were restrained in plastic pipette tips with only the heads protruding. Dental wax was used to secure the animal in the holder and to minimize movements. The brain of the moth was uncovered by opening up a window in the cuticle between the compound eyes and by removing muscles, glands and tracheae. The mouthparts and proboscis were also removed and the brain was constantly rinsed with moth saline (Christensen & Hildebrand, 1987).

Dye loading and optical recording

Retrospective selective staining of PNs was performed by insertion of a dye-coated glass electrode (tip diameter ~10–20 µm) into the inner antennocerebral tract (IACT). The majority of uniglomerular PNs leaving the AL have been shown to exit through the IACT in *S. littoralis* (Anton & Hansson, 1994, 1995; Sadek *et al.*, 2002). Crystals (~200 µg) of FURA-dextran (10 000 MW; Molecular Probes, Eugene, OR, USA) were dissolved in 2 mL bovine serum albumin (~5% solution) and the tip of the electrode was coated with the dye. The level of the moth saline covering the brain was temporarily lowered to prevent the dye from dissolving prior to injection in the brain. To aim for the IACT the electrode was manually inserted close to the midline of the brain about halfway between the AL and the mushroom bodies. The dye was allowed to diffuse for 10–20 s before the electrode was removed. After rinsing with moth saline the preparation was incubated in a cold (8–12 °C) and dark chamber for about 3 h.

To control the distribution of the dye, additional animals were stained with tetramethylrhodamine-dextran (Molecular Probes). The injection procedure was identical to that used for FURA-dextran. In addition, crystals of tetramethylrhodamine-dextran were applied to the AL in order to study the projections of the different antennocerebral tracts. After 3 h of tetramethylrhodamine-dextran loading, the brain was dissected out and fixed in 4% paraformaldehyde overnight. The brain was then washed and dehydrated in a series of stepwise increasing alcohol concentrations. Before scanning, the brain was cleared in methylsalicylate for at least 30 min. The preparations were optically sectioned (~2 µm/section) using a laser scanning confocal microscope (LSM 510 Meta; Zeiss, Germany) with an air Plan-Neofluar objective (20×/0.50). The preparations were excited with a 540-nm laser. Selected sections were further sharpened and contrast enhanced in Adobe Photoshop (v. 7.0).

For imaging we used an air-cooled imaging system (TILL Photonics, Germany) with a 12-bit slow-scan CCD camera. Filter settings were dichroic, 410 nm, emission low pass 440 nm and the preparation was alternately excited at 340 and 380 nm. Exposure times were ~20 and 60 ms, respectively. Sequences of 70 double frames were recorded with a sampling rate of 10 Hz through an upright microscope with a 20× (NA 0.50; Olympus) water immersion objective. On-chip binning (2 × 2) was performed which resulted in a final image size of 320 × 240 pixels. Pixel size at 20× magnification corresponded to ~1 × 1 µm. Execution of protocols and initial analyses of data were performed using the software Till-vision 4,0 (TILL Photonics).

Odorant delivery

A moistened and charcoal-filtered continuous air stream (30 mL/s) ventilated the antenna ipsilateral to the recorded AL through a glass tube (7 mm ID). The glass tube ended ~10 mm from the antenna. An empty

Pasteur pipette attached to a plastic pipette (total volume ~4.5 mL) was inserted through a small hole in the glass tube, blowing an air stream of ~5 mL/s. Another air stream (~5 mL/s) was blown through the odour-loaded pipette by a computer-triggered puffer device (Syntech, the Netherlands) for 1 s (starting at frame 20) into the continuous stream of air. During stimulation the air stream was switched from the empty to the odour-loaded pipette in order to minimize the influence of added air volume. Odorants used in the experiment were 1-octanol, geraniol (+/-)-linalool and phenylacetaldehyde (PAA). The odorants used are biologically relevant to the animal as components of green leaves and flowers of host-plants (Anderson *et al.*, 1993; Jönsson & Anderson, 1999). The purity of the compounds was between 95 and 99%. Odorants were dissolved in paraffin oil. A volume (10 µL) of the solvent containing 50 µg of the respective odorant was applied on filter papers (5 × 15 mm). The filter papers were inserted into Pasteur pipettes, sealed with Para-film (American National Can., Chicago, IL, USA) and stored in a freezer until the start of an experiment. Control stimuli consisted of filter paper with solvent (10 mL) only. Odorants and control were delivered in a randomized order. We allowed at least 60 s between stimulations to reduce adaptation effects.

Data processing

A ratio between the sequences sampled at 340 and 380 nm was first calculated and the ratio-calculated sequences were then spatially median filtered (3 × 3 pixels). For visual presentation of mean responses (Fig. 2) an average of frames 21–30 was calculated and the background was subtracted (mean of frames 7–17). The images were then spatially average filtered (11 × 11 pixels), false-colour coded to the entire intensity range of the strongest responding stimulus and cropped to 75% of maximal activity, i.e. the same scaling was used for all images for easier comparison. For visualization of single images in a sequence (Fig. 4) we subtracted the mean of frames 7–17 from each frame. Each frame was then scaled to its own intensity range. Blank responses (paraffin) evoked negligible responses (Fig. 2) and were not subtracted from odour-evoked responses.

In order to compare activity foci for responses to the odorants across animals we have established a method where we identified the pixel having the strongest change in calcium concentration during odour stimulation (Hansson *et al.*, 2003). We then measured the distance to this coordinate from a midline drawn through the AL and a baseline perpendicular to the midline (see Figure 4a in Hansson *et al.*, 2003). No corrections for variations in the AL size were performed as only minor variations were observed (the width of the ALs differed by less than 10% between individuals, 230–252 mm, mean 242 mm). Furthermore, due to the bottleneck shape at the transition from the AL to the antennal nerve it is difficult to estimate the longitudinal size and thus to normalize the AL size. We then used the coordinates and computed pair-wise comparisons between all of the activity foci of the four odours by means of a multivariate analysis of variance (MANOVA) using the Matlab environment (The Mathworks, Natick, MA, USA). As we performed six comparisons we used a comparison-wise error rate of 0.0085, which amounts to an experiment-wise error rate of 0.05.

For quantitative measurements the frame-wise computed fluorescence value in regions of interest (mean of 10 × 10 pixels, ~10 × 10 µm) in the centre of visible glomeruli (14–18, Fig. 1E) was used as the time course of the response of a certain glomerulus. The size of the regions of interest fits well within the size of a glomerulus (~50 µm) and the position in the centre limited light scattering from neighbouring glomeruli. Smaller regions rendered

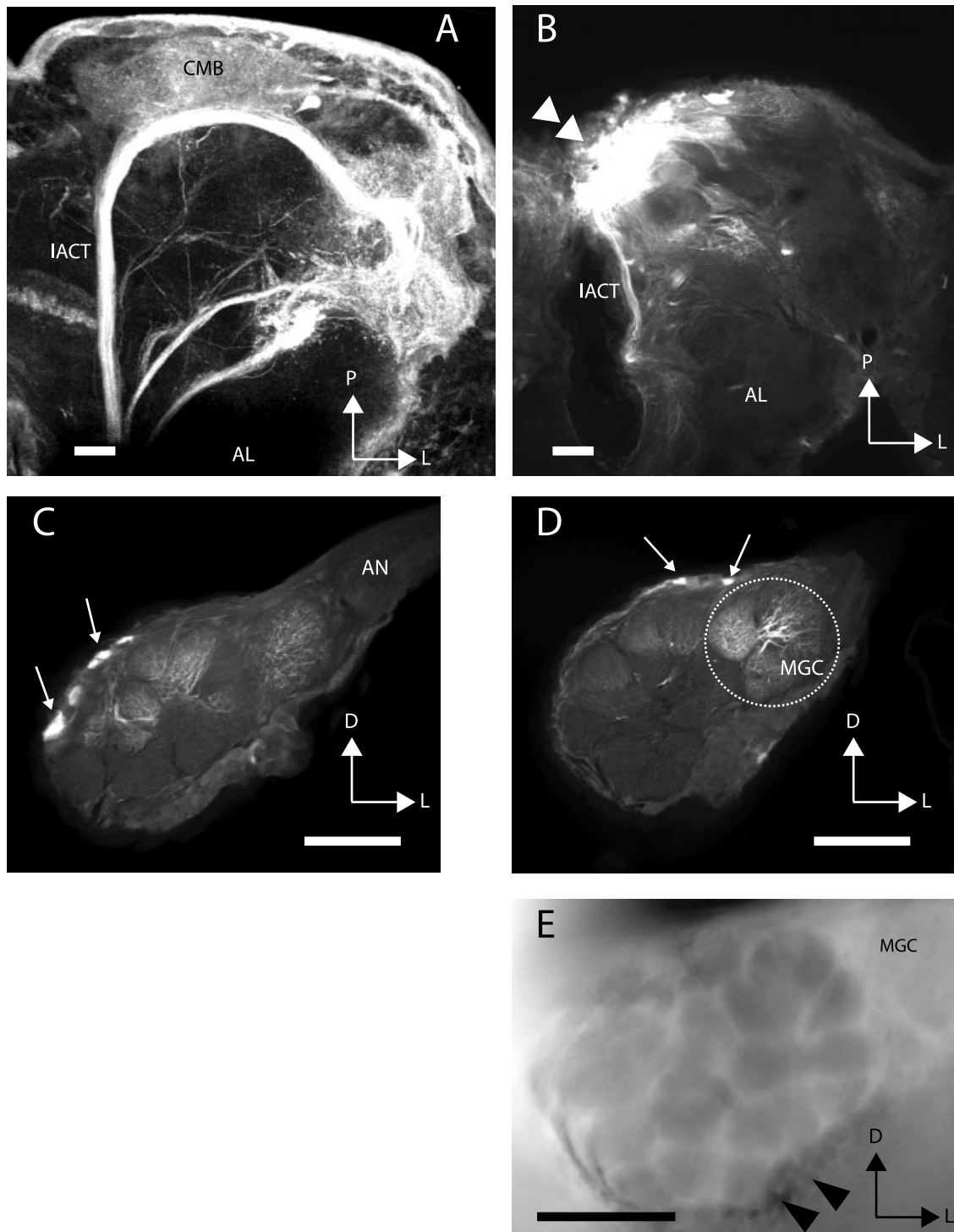
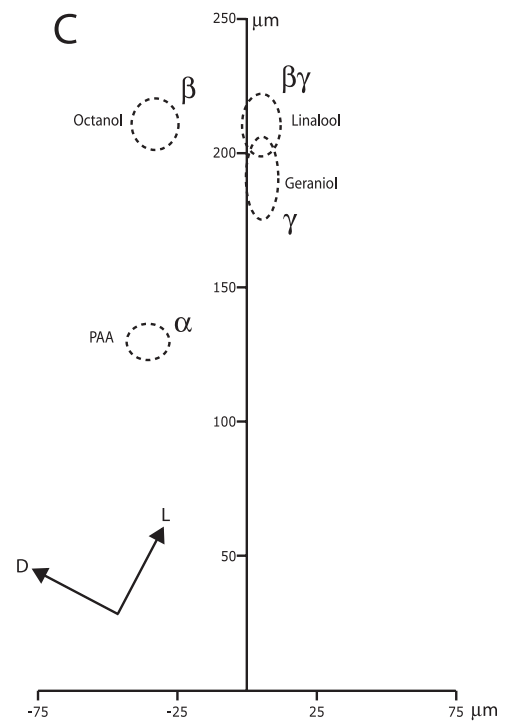
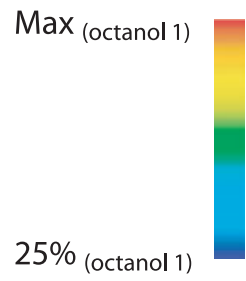
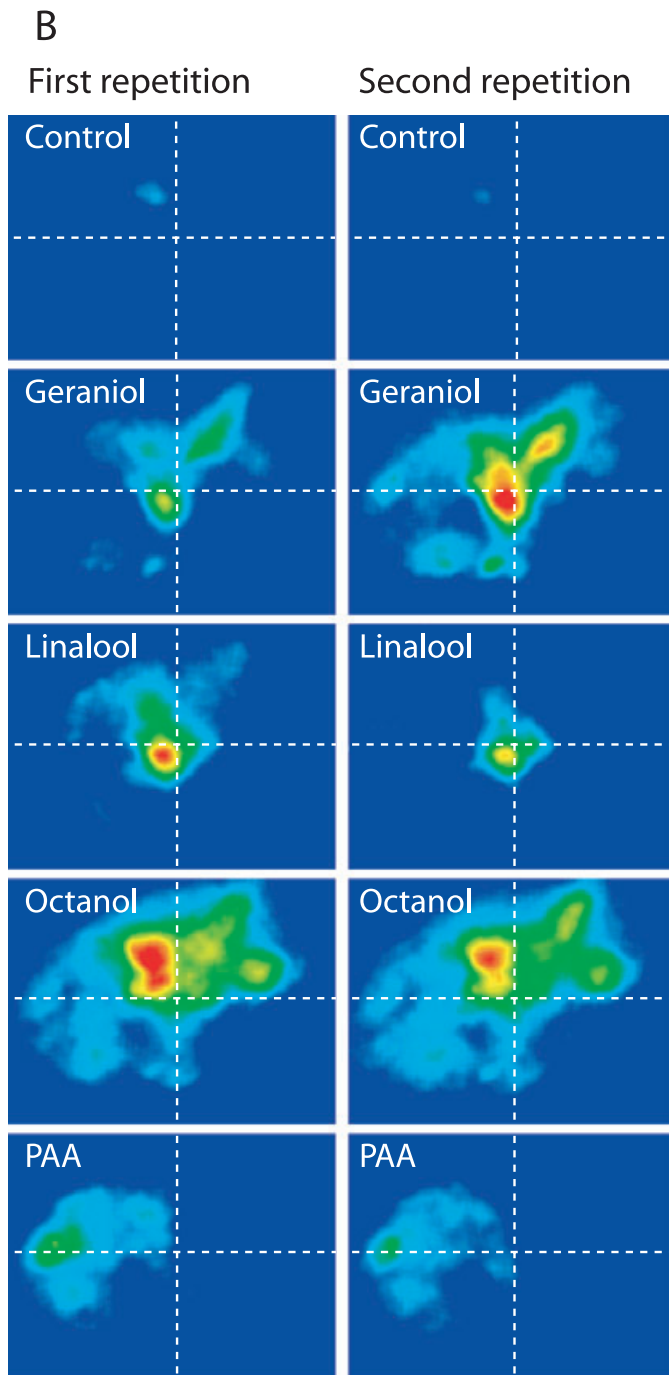
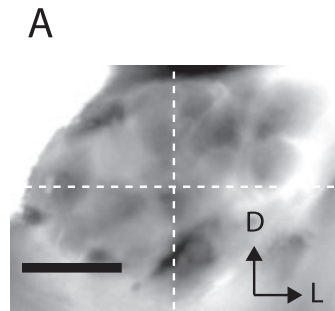


FIG. 1. (A) The different antennocerebral tracts containing projection neurones (PNs) projecting from the antennal lobe (AL) (image kindly provided by Marcus Sjöholm). Crystals of tetramethylrhodamine-dextran were applied in the AL and the dye was allowed to anterogradely diffuse in the PNs to the protocerebrum. In this optical section at least three different tracts can clearly be distinguished, with the inner antennocerebral tract (IACT) as the largest and most conspicuous. (B–D) Retrograde staining of PNs after injection (double arrowhead) with tetramethylrhodamine-dextran in the IACT. The three figures are from different focal depths in the same animal and show the IACT and PN arborizations in different glomeruli. In D the macroglomerular complex (MGC) is indicated by the dotted circle. The arrows point out somata located in the medial cell cluster. (E) A morphological view of the AL after staining with FURA-dextran through the inner antennocerebral tract. The somata (arrowheads) are visible as well as the glomerular outlines. AN, antennal nerve; CMB, calyx of the mushroom body; D, dorsal; L, lateral; P, posterior. Scale bars, 100 μ m.

noisier time courses and larger regions did not further improve the signal-to-noise ratio. To compensate for different background fluorescence we subtracted from each time course its corresponding mean

activity during frames 7–17. All time courses were temporally filtered using a median filter with a length of three frames. This time course will subsequently be called a glomerular response.



A principal component analysis (PCA) was performed to compare the distances between the response vectors to different odours. In this analysis, data from a single animal were used and a response vector to an odour was defined as the spatial vector with as many entries as visible glomeruli where each entry was the mean of the glomerular response over frames 21–30. The response vectors obtained from all repetitions with all odours were written in a response matrix of size (number of glomeruli) \times (total number of stimulations). A PCA was computed based on this response matrix. Additionally, the average response vectors of each odour were tested for significant differences by means of a MANOVA (Matlab).

In order to quantify differences in odour-evoked time courses across glomeruli we compared the glomerular responses to a given odour at three time bins (300, 600 and 900 ms after stimulus onset, respectively) in two different glomeruli. The response amplitudes at these three time bins were statistically analysed by a paired *t*-test.

Finally, we compared activity patterns evoked by different odorants at all time bins after response onset. Between 14 and 18 (mean 16.3) glomeruli were clearly visible in the recordings from different animals. Thus, at each time bin an odour-evoked response was represented by a vector in a 14–18-dimensional space. In each animal we calculated the correlation between the vectors of the same time bin for all odour pairs (Pearson linear test; JMP SAS, Cary, NC, USA). Only animals in which the odours were tested at least twice were used for this analysis. The correlation indices for each odour pair were averaged in each animal. The trial-to-trial correlation indices for the same stimulus were also averaged. We then tested whether the correlation index for a given odour pair (or trial-to-trial with the same odour) changed with time. As correlation indices are usually not normally distributed we used a statistical test (Friedman's test, Matlab) based on rankings of the correlation indices at all time bins from response onset and 1 s onwards. The same analysis was performed in a single animal (with multiple trials, 11–12) to test the consistency across trials. To quantify the change of individual patterns over time we calculated the linear correlation (Pearson) between the glomerular pattern evoked in the first responding frame with the glomerular patterns evoked in each subsequent frame.

Results

Anatomical stainings

Anterograde tetramethylrhodamine-dextran stainings from the AL showed at least three different tracts projecting to either the mushroom bodies or to the lateral protocerebrum (Fig. 1A). The IACT was the largest and most conspicuous of the tracts. Injection of tetramethylrhodamine-dextran into the IACT showed staining of the tract and PNs in the AL (Fig. 1B–D). PN arborizations were observed in both the macroglomerular complex (Fig. 1C) and ordinary glomeruli (Fig. 1D). All anterior glomeruli, which are accessible to optical imaging, had stained PN arborizations.

Retrograde staining of PNs from the IACT with FURA-dextran showed visible somata in the lateral and medial cell clusters (Fig. 1E). Furthermore, the glomerular outlines were often clearly visible and measurements were only made from individual glomeruli seen in these stainings. Neither somata nor glomeruli were visible without staining.

Odour-evoked responses

Odour-evoked signals were observed in 13 animals (out of more than 350 tested animals). In nine of these animals we tested all stimuli at least twice. In one additional animal we tested only octanol and PAA at 12 and 11 repetitions, respectively. The remaining three responding animals did not respond long enough to be used in any analysis. Responses consisted of focal regions of increased fluorescence intensity shortly (100–200 ms) after onset of odour exposure. No inhibitory responses were recorded. In the responding (but not the non-responding) animals we frequently observed spontaneous activity. This activity was much weaker than odour-evoked responses, alternated randomly among glomeruli and had short durations (100–300 ms). Odour-evoked activity was easily discerned from spontaneous activity due to the reproducibility.

We looked at the pure spatial distribution of odour-evoked responses. Glomerular representations were odour dependent and reproducible with repeated stimulations (Fig. 2). For instance, we observed clearly delineated and slightly overlapping response maps for geraniol, linalool, octanol and PAA. In this example both geraniol and linalool strongly activated a centrally located glomerulus. Geraniol, however, additionally evoked a strong response in an elongated region located dorso-laterally from the former. This region was also moderately activated by octanol. Octanol, on the other hand, elicited the strongest response in a glomerulus located dorsally to that activated by geraniol and linalool. The relative locations of the key glomeruli persisted across animals ($n = 9$). The coordinates for the activity foci evoked by the different odours were compared across animals. In Fig. 2C the distances to the coordinates were averaged across animals. A MANOVA test (confidence level 0.0085) comparing the six combinations of the four coordinates revealed that all pairs of activity foci except geraniol–linalool ($P = 0.620$) and linalool–octanol ($P = 0.018$) differed significantly (geraniol–octanol, $P = 0.0063$; geraniol–PAA, $P = 6.04 \times 10^{-5}$; linalool–PAA, $P = 1.40 \times 10^{-5}$; octanol–PAA, $P = 2.62 \times 10^{-5}$).

In addition to the most strongly activated glomerulus we wanted to investigate the persistence of the global patterns of glomerular activity averaged over the entire stimulus period. We performed a PCA in a single animal (four to five repetitions of each odour stimulus). A response pattern to an odour is defined as a spatial vector where the response amplitude in each visible glomerulus (14 glomeruli) represented a single dimension (see Materials and methods). Figure 3A shows a graphic representation of the first three principal components, which describe 92.6% of the total variance of the data (Fig. 3C), and the coordinates of the first three principal components are shown in Fig. 3B. Using a comparison of the between-groups distance to the within-groups distance (Knüsel *et al.*, 2004), we observed that only the first three principal components described group-specific information, i.e. the between-distance was larger than the within-distance for the first three dimensions (Fig. 3D). The organization of the response patterns in this three-dimensional PCA space showed that the responses to octanol and PAA were clearly separated and narrowly clustered. The spatial organization of the responses to geraniol and linalool grouped in less defined clusters but were separated from octanol and PAA. Geraniol and linalool are two plant-derived monoterpenes with the same chemical composition and are structural

Fig. 2. Odour-evoked Ca^{2+} responses in a single animal. (A) A grayscale image of the antennal lobe showing the area from which recording was made. (B) False-colour coded responses to a control (paraffin oil) and four different plant-associated compounds (two repetitions). Frames are averaged around the peak of activity (frames 21–30) and background activity (frames 7–17) was subtracted. The image showing the response to the first stimulation with octanol (the strongest response in the panel) was scaled to its own intensity range and clipped to the upper 75% of activity. The same intensity scale was then used for all images. (C) The coordinates (mean \pm SEM, $n = 9$) for the response foci evoked by the four odorants. Different labels represent significantly different locations. The stimulus dose is 50 μg for all compounds. D, dorsal; L, lateral; PAA, phenylacetaldehyde. Scale bar, 100 μm .

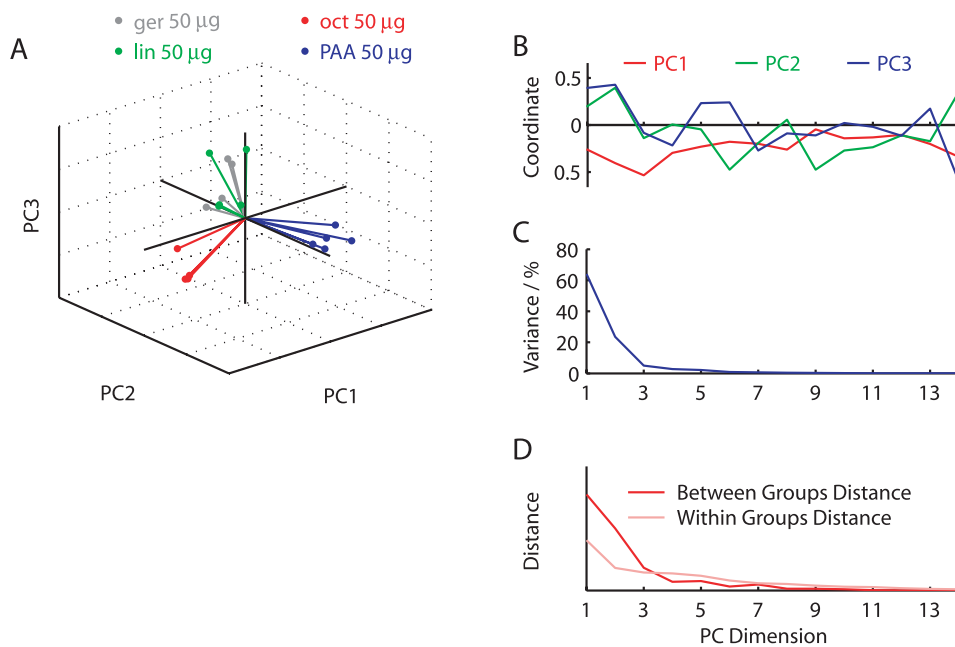


FIG. 3.

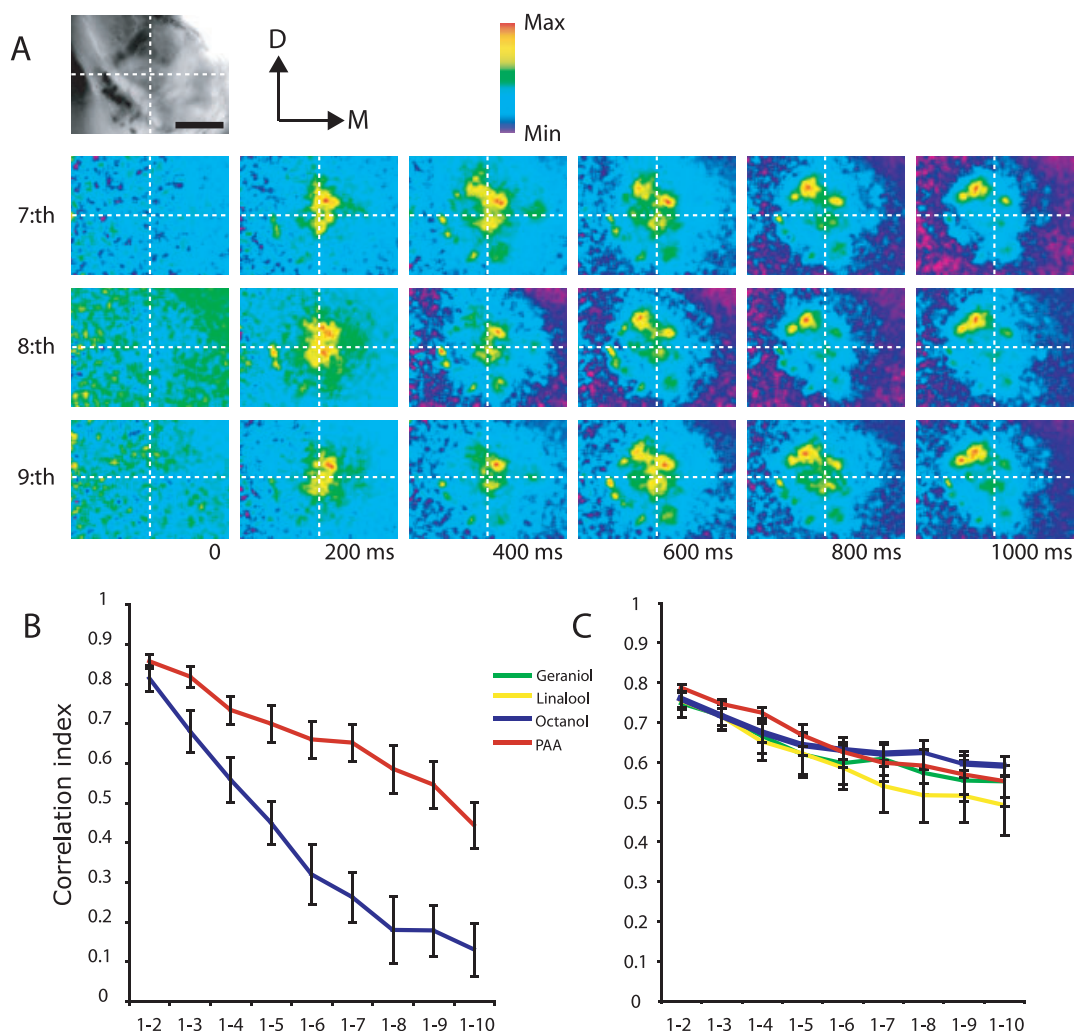


FIG. 4.

isomers of each other. Finally, a MANOVA showed that the multivariate means of the response vectors are different between odours (one-way MANOVA, $\chi^2(42) = 119.2$, $P = 2.5 \times 10^{-9}$; see Materials and methods). Thus, the mean responses are repeatable for the same stimulus and different between stimuli.

Dynamics of spatial activity patterns

In addition to the stimulus-dependent spatial organization of the PN responses we also observed that the activity patterns showed a temporal evolution. For instance, when we considered the response sequence to octanol the focus of activity moved in a lateral direction and this dynamical response was consistent across repetitions ($n = 12$ trials; Fig. 4). In the same animal we calculated the linear correlation (Pearson) between the activity patterns evoked by either octanol or PAA at the first responding frame with the patterns evoked at all consecutive frames 900 ms onwards. We found that the similarity decreased with increasing temporal distance between the frames ($P \ll 0.001$ for both odours; Friedman's test; $n = 12$ trials with octanol and 11 trials with PAA). The same kind of analysis was performed across all animals. In each animal the correlation pairs were first averaged. For all four odours the decrease in similarity was significant ($P \ll 0.001$ for all odours; Friedman's test; $n = 9$ animals).

We found that when comparing the response amplitude in different glomeruli at different time bins their relative strength differed (Fig. 5). The responses of two arbitrary glomeruli showed consistent temporal dynamics across trials. For instance, glomerulus number 2 showed a stronger response to octanol 300 ms after stimulus onset compared with glomerulus number 1. At about 600 ms the time courses crossed and at 900 ms the activation of glomerulus 1 exceeded that of glomerulus 2. These differences in response amplitude were statistically significant at 300 and 900 but not at 600 ms (paired t -test, one-sided at 300 and 900 ms, two-sided at 600 ms, $P = 0.018$, $P = 0.88$, $P = 0.00003$, respectively, $n = 12$). For PAA, on the other hand, the strongest activity was recorded in glomerulus 2 at all three time bins ($P \ll 0.001$ at all three time bins, $n = 11$). Hence, temporal response modulations are dependent on both stimulus and glomerulus.

Similarity reduction of activity patterns evoked by different odours

Finally, we wanted to examine whether the similarity of the spatial patterns evoked by different odorants changed during the course of odour stimulation. We calculated the linear correlation (Pearson linear test) at each time bin between all pairs of activity patterns, both in a

single animal (Fig. 6A) with multiple trials of two of the odours and across nine animals where we had obtained at least two repetitions of all four odours (Fig. 6B). The correlations were calculated for all time bins in a sequence. The correlations obtained at the different time bins from response onset (300 ms after stimulus onset) and 900 ms onwards were compared in a statistical test (Friedman's test; Matlab). As a control we compared trial-to-trial correlations of patterns evoked by the same odour (all odours pooled). The latter correlations did not significantly change over time ($P = 0.14$ in the single animal and $P = 0.64$ across all animals). Correlations of responses evoked by different odorants, on the other hand, changed as a function of time (with one exception). The similarity between the responses decreased from 300 to 1200 ms after stimulus onset. Responses to geraniol and octanol also decreased in similarity but, due to a high variance, the difference was not statistically significant ($P = 0.06$). This analysis demonstrates a temporal sharpening of the spatial response patterns in the sense that the similarity of the patterns evoked by different odours decreased with time.

Discussion

We investigated the spatial and temporal organization of the dynamics of the intracellular Ca^{2+} concentration in a large population of PNs in response to plant odour stimulation in the moth *S. littoralis*. We showed that FURA-dextran labelling via the IACT gives a PN-specific staining that allows imaging of spatio-temporal responses at moderately high resolutions. Using this method we have observed repeatable responses to the odour stimulation that displayed a consistent spatio-temporal organization of the PN Ca^{2+} dynamics. Moreover, we showed that the PN responses triggered by different stimuli became increasingly more decorrelated with time.

A spatial representation of odours in the AL (or olfactory bulb) is the consequence of the organization of converging ORNs (Gao *et al.*, 2000; Vosshall *et al.*, 2000). This spatial organization is at least roughly conserved at the output level. When we averaged the Ca^{2+} responses over the entire stimulus period, we found that the odours evoked spatially specific patterns of glomerular activation that were repeatable across stimulations. An analysis of coordinates of activity foci revealed that the relative locations of certain key glomeruli were conserved across animals. The same relative locations were observed at the input level (Carlsson *et al.*, 2002; Carlsson & Hansson, 2003). In the honeybee, Sachse & Galizia (2002) further showed that, even though the strongest responding glomeruli were the same, the contrast between the global patterns evoked by different odours increased from input to output, which suggests the action of an inhibitory network.

A PCA analysis of the global activity patterns averaged over the entire stimulus window revealed that the spatial representation of the

FIG. 3. Principal component analysis of the spatial response vectors (responses in 14 glomeruli) to four different odours (four or five trials with each odour) in a single animal. (A) Representations of odours in the space formed by the first three principal components. (B) The coordinates of the first three basis vectors of the principal component system. (C) Percentage of variance explained vs. principal component dimension. (D) Comparison of the within- to the between-group distance as a function of the principal component dimension. The between-groups distance is the average distance between the centres of the clusters formed by each odour computed for each PC dimension. Similarly, the within-groups distance is the average size of each cluster along every principal component dimension. ger, geraniol; lin, linalool; oct, octanol; PAA, phenylacetaldehyde.

FIG. 4. Activation patterns are dynamic. (A) False-colour coded images of responses to octanol (three repetitions, 7th, 8th and 9th). Every second frame is shown starting at the stimulus onset (time 0). Each frame is scaled to its own intensity range. The focus of activity is moving between glomeruli and the sequencing is reproducible across repetitions. The grayscale image shows the antennal lobe used for recordings. D, dorsal; M, medial. Scale bar, 100 μm . Time after stimulus onset is indicated. (B) Correlation indices for the comparisons between the first frame showing a clear response and nine consecutive frames in a single animal [mean \pm SEM; $n = 12$, octanol and 11, phenylacetaldehyde (PAA)]. (C) Correlation indices for the comparisons between the first frame showing a response and nine consecutive frames across animals.

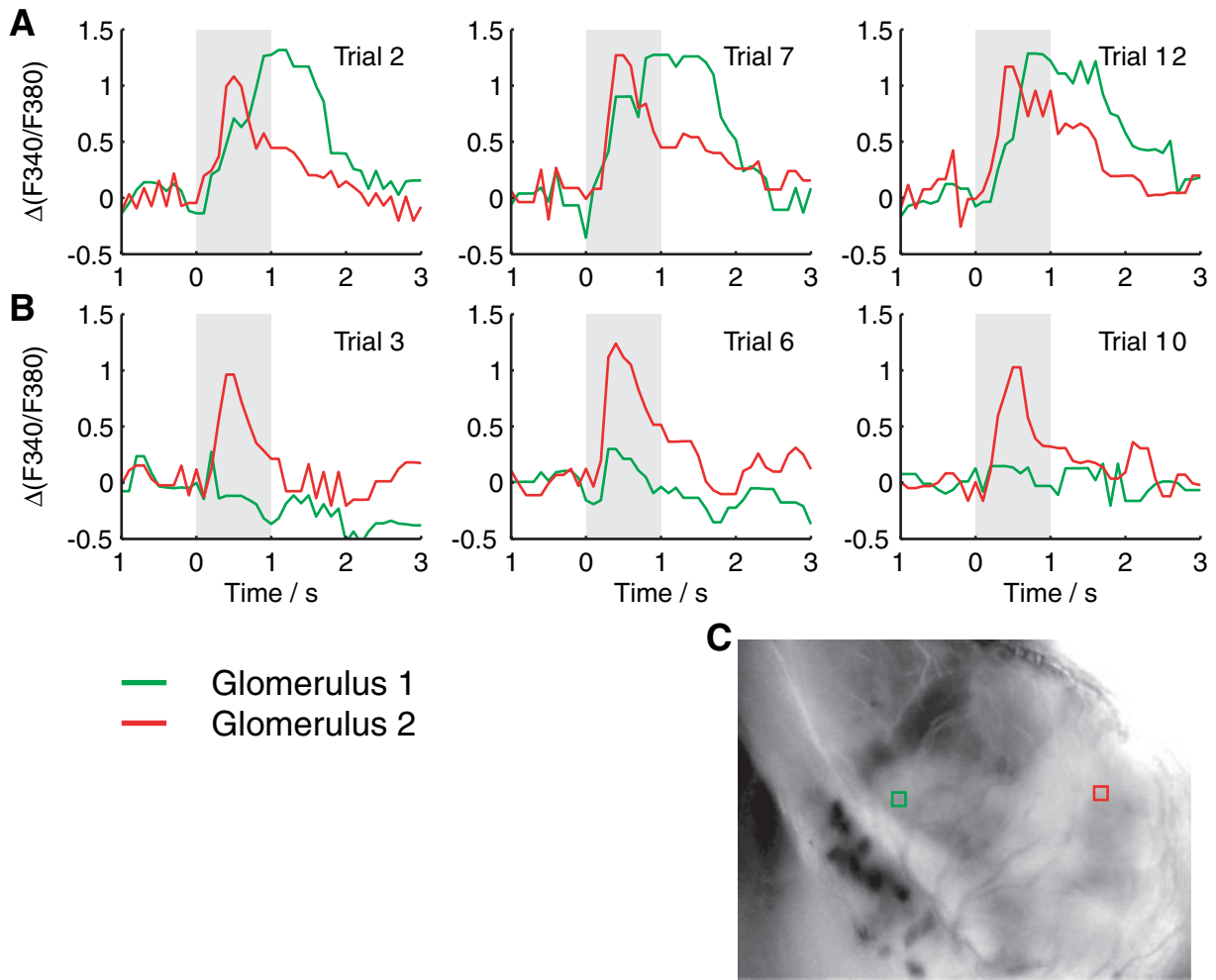


FIG. 5.

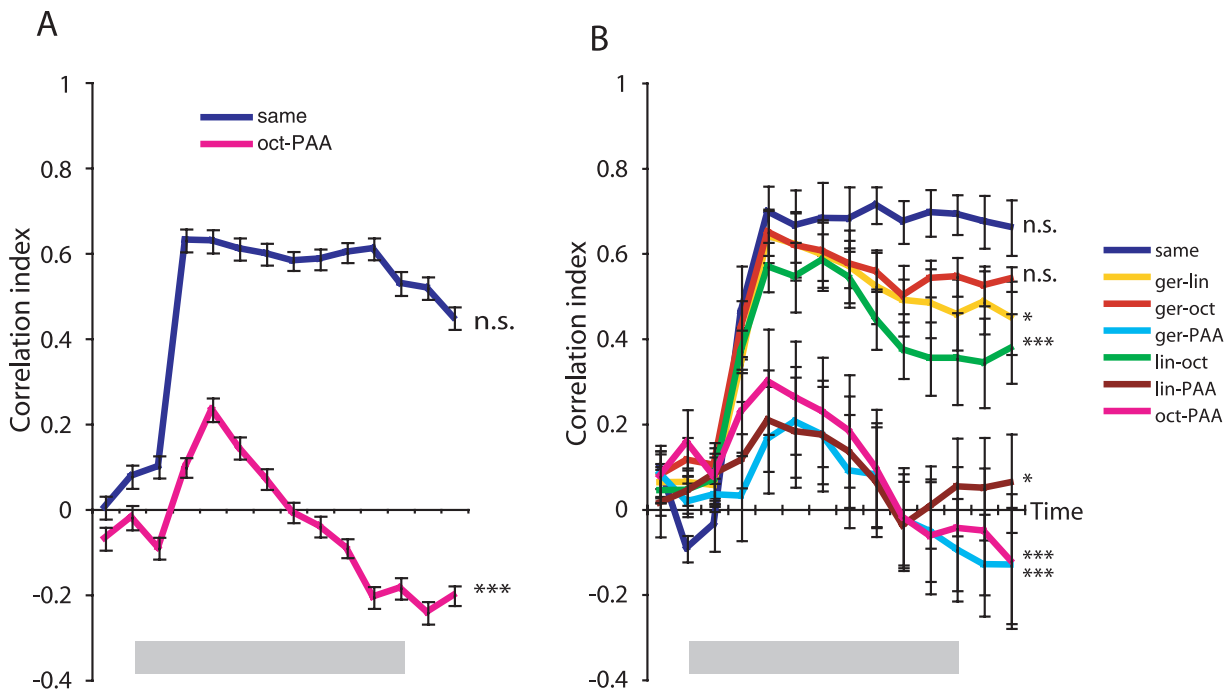


FIG. 6.

odours grouped into clusters. Interestingly, the spatial response patterns evoked by the structurally similar compounds linalool and geraniol were less distinguishable. It should, however, be noted that recordings were performed from a subset of glomeruli (~30%) and if we could include responses in non-accessible glomeruli, the response patterns evoked by similar compounds might differ more clearly.

All responses in our recordings were excitatory. In contrast, Sachse & Galizia (2002) observed inhibitory responses in certain glomeruli in the honeybee to some stimuli. This discrepancy could be due to the fact that different antennocerebral tracts were labelled and these tracts contain PNs with different physiological properties (Müller *et al.*, 2002). Furthermore, different panels of odours were tested and the stimulus time differed.

Similar to other functional imaging studies (Galizia *et al.*, 2000; Sachse & Galizia, 2002; Spors & Grinvald, 2002) we found that glomerular activity patterns were not static during the stimulus presentation. The Ca^{2+} dynamics were temporally complex, glomerulus specific and highly repeatable. All glomeruli responded with a transient increase in Ca^{2+} concentration at about 100–200 ms after stimulus onset. This response latency is consistent with single cell recordings from ORNs and AL neurones in *S. littoralis* using the same odour delivery system as used in the current study (Anton & Hansson, 1994, 1995; Anderson *et al.*, 1995). A large part of this response latency is due to the delivery method, i.e. the time from triggering the puffer device until the molecules reach the receptor site. A stimulus-dependent temporal variability of the PN responses was observed in the decay to baseline. For example, PNs that showed a higher peak amplitude could show a rapid decay and vice versa. As a result the relative relation between amplitudes across PNs changed, which means that the global glomerular activity patterns changed. If duration and intensity were correlated with each other then spatial patterns would be similar at different time points and only differ in absolute strength. Hence, our data suggest that the amplitude time course of the PN Ca^{2+} response might be independently modulated. We are currently investigating this possibility and its implications for the encoding and classification of odour stimuli (Knüsel *et al.*, in preparation). The different shapes of the odour-evoked Ca^{2+} dynamics probably reflect slow temporal patterns of action potentials in individual neurones. Intracellular recordings from single PNs in *S. littoralis* have shown a great variety of temporal patterns, from transient bursts of action potentials, multiphasic responses, to tonic responses that outlast the stimulus (Anton & Hansson, 1994, 1995; Sadek *et al.*, 2002). It is not likely that the slow temporal patterns of PN responses are driven by direct input from the ORNs. The ORNs in *S. littoralis* generally respond to olfactory cues with rather stereotypical simple firing patterns (Anderson *et al.*, 1995; Jönsson & Anderson, 1999). It is more likely that the slow temporal patterns are the result of collateral processes in the AL. Most local interneurons in the moth AL are GABA-ergic and can potentially modulate the spiking patterns in the PNs by reciprocal interactions between the glomeruli during the course of odour exposure (Tolbert & Hildebrand, 1981; Waldrop *et al.*, 1987; Christensen *et al.*, 1993,

1998; Distler & Boeckh, 1997). Indeed, Sachse & Galizia (2002) found evidence that application of picrotoxin, which antagonizes GABA-gated Cl^- channels, changed the temporal patterns of PN activity in the honeybee. In contrast, picrotoxin had no effect on slow temporal patterns in single PNs in honeybees or locusts (MacLeod & Laurent, 1996; Stopfer *et al.*, 1997; MacLeod *et al.*, 1998). However, coherent spiking activity between pairs of PNs and oscillations caused by neural synchrony was abolished. Coherent spiking activity has been shown to carry further information about odour identity and abundance (Wehr & Laurent, 1996; Christensen *et al.*, 2000; Lei *et al.*, 2004). Lei *et al.* (2004) further showed that the pure spatial identity of activated AL neurones in a moth was sufficient (for the observer) to discriminate between structurally different compounds, whereas temporal patterns of coherent activity provided additional information that made it possible to discriminate even structurally similar odorants. In honeybees, abolishment of neural synchrony led to a substantially reduced ability to behaviourally discriminate similar but not dissimilar odours (Stopfer *et al.*, 1997). Moreover, blocking the synchronized PN activity in locusts resulted in a broadened tuning of the PN target cells, the Kenyon cells in the mushroom bodies (Perez-Orive *et al.*, 2004).

Friedrich & Laurent (2001, 2004) showed that mitral cell firing patterns evoked by different odours in zebrafish decorrelated over time. Individual mitral cell response profiles remained, on average, constant, i.e. tuning did not narrow over time while the overlap of responding neurones decreased. Similarly, recordings from AL neurones in locusts and moths have demonstrated a temporally enhanced contrast between patterns of coherent activity evoked by different compounds (Stopfer *et al.*, 2003; Daly *et al.*, 2004). Inspired by these studies we set out to investigate how correlations between odour-evoked global activity patterns of PNs changed during the course of odour exposure. We found that representations of different compounds became increasingly more decorrelated with time. The correlations between patterns evoked by the same odour, however, did not change significantly during the course of stimulation. This control showed that this result was not due to an increase of noise in the signals during the period of stimulation and that the spatio-temporal patterns were reproducible. Three of the odorants used (geraniol, linalool and octanol) elicited glomerular activity patterns that were highly correlated shortly after response onset. These three compounds are indeed structurally similar. The two monoterpenes, geraniol and linalool, for example, are structural isomers of each other. In contrast, responses to PAA, an aromatic compound with an attached aldehyde group, clearly already differed from responses to the other compounds at the response onset. Geraniol, linalool and octanol activate overlapping subsets of ORNs in *S. littoralis* (Anderson *et al.*, 1995; Jönsson & Anderson, 1999). PAA and other aromatic compounds, on the other hand, activate different subsets of ORNs. Regardless of the original similarity, patterns evoked by different compounds sharpened during the course of exposure. This observation raises the question as to what the behavioural significance would be for the temporal improvement of odour representations. One could speculate that the initial encounter with plant-related volatiles may only require increased attention and a rough discrimination. As the moth approaches a potential

FIG. 5. Calcium dynamics for (A) octanol and (B) phenylacetaldehyde (PAA) measured in two glomeruli (see map, C). Three repetitions of each are shown. The shaded areas indicate the stimulus period (1 s). With octanol glomerulus 2 consistently reaches the response peak before glomerulus 1. With PAA, on the other hand, glomerulus 2 always responds most strongly. See the text for statistical analyses.

FIG. 6. (A) Correlation indices (mean \pm SEM) for comparisons of responses evoked by either the same odour [octanol or phenylacetaldehyde (PAA), 132 comparisons] or between odours (octanol and PAA, 121 comparisons) in a single animal at each 100-ms bin. (B) Average correlation index (Pearson linear test) for each pair of odours across animals (\pm SEM; $n = 9$ animals) calculated for each 100-ms bin. In the across trial comparison, correlations of all pairs of the same odour were averaged. The grey bars indicate the stimulus window (1 s). * $P < 0.05$; *** $P < 0.001$; n.s., not significant. ger, geraniol; lin, linalool; oct, octanol.

food-source there will be enough time to develop a fine discrimination. Behavioural support for our results comes from the honeybee. Honeybees can easily discriminate between structurally similar compounds (Laska *et al.*, 1999). Correct discrimination, however, required about 700 ms (Ditzen *et al.*, 2003). In the latter study different blend ratios of nonanol and linalool were used, i.e. two straight-chained molecules with attached alcohol group. In our study we also found a high initial similarity between, for example, linalool and octanol which, however, decreased over time. It would thus be very interesting to test the behavioural discrimination time between compounds that are structurally very different, like aromatics and terpenes. Faster discrimination times have been reported from rats (200–300 ms; Uchida & Mainen, 2003; Abraham *et al.*, 2004) whereas humans may need as long as 2 s to discriminate between similar odours (Wise & Cain, 2000). The rats, however, needed several hundred trials to learn the fast discrimination (Abraham *et al.*, 2004). Discrimination improvement would probably not work in the moth pheromone-detecting subsystem. The reaction time of the male moth to the female-emitted sex pheromone can be as fast as 150 ms (Baker & Haynes, 1987). Furthermore, pheromone-sensitive PNs can resolve repetitive stimulation up to 10 Hz (Christensen & Hildebrand, 1988). Different components of the sexual pheromone are processed in discrete units of the macroglomerular complex (Hansson, 1997) and response optimization may neither be necessary nor possible.

We have shown here that the odour identity affects the temporal evolution of the spatial activity patterns. However, other parameters such as stimulus concentration, context and experience may also have an impact on the slow temporal patterns.

A pure spatial coding mechanism may be sufficient to roughly classify odours, i.e. odours belonging to structurally different classes, like terpenes and aromatics. The terpenes used in our study activate overlapping subsets of ORNs (Anderson *et al.*, 1995). Glomeruli receiving input from ORNs responding to terpenes are clustered in the lateral region of the AL, whereas glomeruli representing aromatics are clustered in the medial region in *S. littoralis* (Carlsson *et al.*, 2002; Carlsson & Hansson, 2003) and in *M. sexta* (Hansson *et al.*, 2003). In *M. sexta*, this organization is also conserved at the output level (Lei *et al.*, 2004). Using a multiprobe electrode Lei *et al.* (2004) demonstrated that, for example, aromatics and terpenes could easily be discriminated simply by the location of the responding electrodes. Two structurally similar terpenes, linalool and nerol, however, could only be distinguished when the temporal patterns of coherent activity among the responding neurones were considered. Using a much longer stimulation time (1000 ms compared with 100 ms in the study by Lei *et al.* 2004) we further showed a temporal change in spatial patterns and the discrimination of odour identity based on these patterns improved with time. It would thus be very interesting to see whether fine-odour classification by coherent activity further improves by the action of the slow temporal patterns. Indeed, Daly *et al.* (2004) showed when using a multiprobe electrode in *M. sexta* that the distance between responses to any two odorants reached a maximum at about 240 ms. However, as the stimulus time was only 200 ms it is likely that a sustained stimulation would further improve the discrimination ability.

The decorrelation is probably caused by the action of a lateral inhibitory network. However, before experimental testing we cannot exclude the possibility that it is driven directly by afferent input. In future experiments we plan to combine optical imaging with electrophysiology in order to confirm the relation between optical signals and characteristics of individual neurones and also to apply pharmacological treatments in an attempt to reveal the mechanism behind the temporal sharpening of activity patterns.

We have shown that the spatial odour-evoked activity in a large population of PNs is dynamic and that the contrast between responses to different odours increases over time. Our results suggest that if the moth uses a spatial olfactory code for recognition and discrimination, this code is dynamic and 'improves' during the course of odour exposure. Thus, a hierarchical coding scheme may exist where a rough classification of chemical structures can be performed shortly after response onset. With time, however, a decorrelation takes place between responses evoked by similar as well as dissimilar odours.

Acknowledgements

We thank Jan-Eric Englund for expert statistical advice and Rickard Ignell and Sylvia Anton for valuable comments on the manuscript. Thanks to Giovanni C. Galizia and Silke Sachse for teaching us how to load the dye. We gratefully acknowledge support by the EU (grant EU-FET AMOTH IST-2001-33066) and the Swedish Research Council.

Abbreviations

AL, antennal lobe; IACT, inner antennocerebral tract; MANOVA, multivariate analysis of variance; ORN, olfactory receptor neurone; PAA, phenylacetaldehyde; PCA, principal component analysis; PN, projection neurone.

References

- Abraham, N.M., Spors, H., Carleton, A., Margrie, T.W., Kuner, T. & Schaefer, A.T. (2004) Maintaining accuracy at the expense of speed: stimulus similarity defines odor discrimination time in mice. *Neuron*, **44**, 865–876.
- Anderson, P., Hilker, M., Hansson, B.S., Bombosch, S., Klein, B. & Schildknecht, H. (1993) Oviposition deterring components in larval frass of *Spodoptera littoralis* (Boisd.) (Lepidoptera: Noctuidae): a behavioural and electrophysiological evaluation. *J. Insect Physiol.*, **39**, 129–137.
- Anderson, P., Hansson, B.S. & Löfqvist, J. (1995) Plant-odour-specific receptor neurons on the antennae of the female and male *Spodoptera littoralis*. *Physiol. Entomol.*, **20**, 189–198.
- Anton, S. & Hansson, B.S. (1994) Central processing of sex pheromone, host odour, and oviposition deterrent information by interneurons in the antennal lobe of female *Spodoptera littoralis* (Lepidoptera: Noctuidae). *J. Comp. Neurol.*, **350**, 199–214.
- Anton, S. & Hansson, B.S. (1995) Sex pheromone and plant-associated odour processing in antennal lobe interneurons of male *Spodoptera littoralis* (Lepidoptera: Noctuidae). *J. Comp. Physiol. A*, **176**, 773–789.
- Anton, S. & Homberg, U. (1999) Antennal lobe structure. In Hansson, B.S. (Ed.), *Insect Olfaction*. Springer, Berlin, pp. 97–124.
- Baker, T.C. & Haynes, K.F. (1987) Manoeuvres used by flying male oriental fruit moths to relocate a sex pheromone plume in an experimentally shifted wind-field. *Physiol. Entomol.*, **12**, 263–279.
- Carlsson, M.A. & Hansson, B.S. (2003) Dose–response characteristics of glomerular activity in the moth antennal lobe. *Chem. Senses*, **28**, 269–278.
- Carlsson, M.A., Galizia, C.G. & Hansson, B.S. (2002) Spatial representation of odours in the antennal lobe of the moth *Spodoptera littoralis* (Lepidoptera: Noctuidae). *Chem. Senses*, **27**, 231–244.
- Christensen, T.A. & Hildebrand, J.G. (1987) Male-specific, sex pheromone-selective projection neurons in the antennal lobes of the moth *Manduca sexta*. *J. Comp. Physiol. A*, **160**, 553–569.
- Christensen, T.A. & Hildebrand, J.G. (1988) Frequency coding by central olfactory neurons in the sphinx moth *Manduca sexta*. *Chem. Senses*, **13**, 123–130.
- Christensen, T.A., Waldrop, B.R., Harrow, I.D. & Hildebrand, J.G. (1993) Local interneurons and information processing in the olfactory glomeruli of the moth *Manduca sexta*. *J. Comp. Physiol. A*, **173**, 385–399.
- Christensen, T.A., Waldrop, B.R. & Hildebrand, J.G. (1998) GABAergic mechanisms that shape the temporal response to odors in the moth olfactory projection neurons. *Ann. N.Y. Acad. Sci.*, **855**, 475–481.
- Christensen, T.A., Pawlowski, V.M., Lei, H. & Hildebrand, J.G. (2000) Multi-unit recordings reveal context-dependent modulation of synchrony in odor-specific neural ensembles. *Nat. Neurosci.*, **3**, 927–931.
- Daly, K.C., Wright, G.A. & Smith, B.H. (2004) Molecular features of odorants systematically influence slow temporal responses across clusters of

- coordinated antennal lobe units in the moth *Manduca sexta*. *J. Neurophysiol.*, **92**, 236–254.
- Distler, P.G. & Boeckh, J. (1997) Synaptic connections between identified neuron types in the antennal lobe glomeruli of the cockroach, *Periplaneta americana*. II. Local multiglomerular interneurons. *J. Comp. Neurol.*, **383**, 529–540.
- Ditzen, M., Evers, J.F. & Galizia, C.G. (2003) Odor similarity does not influence the time needed for odor processing. *Chem. Senses*, **28**, 781–789.
- Friedrich, R.W. & Laurent, G. (2001) Dynamic optimization of odor representations by slow temporal patterning of mitral cell activity. *Science*, **291**, 889–894.
- Friedrich, R.W. & Laurent, G. (2004) Dynamics of olfactory bulb input and output activity during odor stimulation in zebrafish. *J. Neurophysiol.*, **91**, 2658–2669.
- Galizia, C.G., Küttner, A., Joerges, J. & Menzel, R. (2000) Odour representation in the honeybee olfactory glomeruli shows slow temporal dynamics: an optical recording study using a voltage-sensitive dye. *J. Insect Physiol.*, **46**, 877–886.
- Galizia, G.G., Sachse, S., Rappert, A. & Menzel, R. (1999) The glomerular code for odor representation is species specific in the honeybee *Apis mellifera*. *Nat. Neurosci.*, **2**, 473–478.
- Gao, Q., Yuan, B. & Chess, A. (2000) Convergent projections of *Drosophila* olfactory neurons to specific glomeruli in the antennal lobe. *Nat. Neurosci.*, **3**, 780–785.
- Hansson, B.S. (1997) Antennal lobe projection patterns of pheromone-specific olfactory receptor neurons in moths. In Cardé, R.T. & Minks, A.K. (Eds), *Insect Pheromone Research: New Directions*. Chapman & Hall, New York, pp. 164–183.
- Hansson, B.S., Carlsson, M.A. & Kalinová, B. (2003) Olfactory activation patterns in the antennal lobe of the sphinx moth, *Manduca sexta*. *J. Comp. Physiol. A*, **189**, 301–308.
- Hinks, C.F. & Byers, J.R. (1976) Biosystematics of the genus *Euxoa* (Lepidoptera: Noctuidae). V. Rearing procedures and life cycles of 36 species. *Can. Entomol.*, **108**, 1345–1357.
- Johnson, B.A., Woo, C.C. & Leon, M. (1998) Spatial coding of odorant features in the glomerular layer of the rat olfactory bulb. *J. Comp. Neurol.*, **393**, 457–471.
- Jönsson, M. & Anderson, P. (1999) Electrophysiological response to herbivore-induced host plant volatiles in the moth *Spodoptera littoralis*. *Physiol. Entomol.*, **24**, 377–385.
- Kauer, J.S. & White, J. (2001) Imaging and coding in the olfactory system. *Ann. Rev. Neurosci.*, **24**, 963–979.
- Knüsel, P., Wyss, R., König, P. & Verschure, P.F.J.M. (2004) Decoding a temporal population code. *Neural Comput.*, **16**, 2079–2100.
- Laska, M., Galizia, C.G., Giurfa, M. & Menzel, R. (1999) Olfactory discrimination ability and odor structure-activity relationships in honeybees. *Chem. Senses*, **24**, 429–438.
- Laurent, G. (2002) Olfactory network dynamics and the coding of multidimensional signals. *Nat. Rev. Neurosci.*, **3**, 884–895.
- Laurent, G., Wehr, M. & Davidowitz, H. (1996) Temporal representations of odors in an olfactory network. *J. Neurosci.*, **16**, 3837–3847.
- Laurent, G., Stopfer, M., Friedrich, R.W., Rabinovich, M.I., Volkovskii, A. & Abarbanel, H.D. (2001) Odor encoding as an active, dynamical process: experiments, computation, and theory. *Annu. Rev. Neurosci.*, **24**, 263–297.
- Lei, H., Christensen, T.A. & Hildebrand, J.G. (2004) Spatial and temporal organization of ensemble representations for different odor classes in the moth antennal lobe. *J. Neurosci.*, **24**, 11 108–11 119.
- MacLeod, K., Backer, A. & Laurent, G. (1998) Who reads temporal information contained across synchronized and oscillatory spike trains? *Nature*, **395**, 693–698.
- MacLeod, K.M. & Laurent, G. (1996) Distinct mechanisms for synchronization and temporal patterning of odor-encoding neural assemblies. *Science*, **274**, 976–979.
- Meijerink, J., Carlsson, M.A. & Hansson, B.S. (2003) Spatial representation of odorant structure in the moth antennal lobe: a study of structure response relationships at low doses. *J. Comp. Neurol.*, **467**, 11–21.
- Müller, D., Abel, R., Brandt, R., Zöckler, M. & Menzel, R. (2002) Differential parallel processing of olfactory information in the honeybee, *Apis mellifera* L. *J. Comp. Physiol. A*, **188**, 359–370.
- Perez-Orive, J., Bazhenov, M. & Laurent, G. (2004) Intrinsic and circuit properties favor coincidence detection for decoding oscillatory input. *J. Neurosci.*, **24**, 6037–6047.
- Sachse, S. & Galizia, C.G. (2002) Role of inhibition for temporal and spatial odor representation in olfactory output neurons: a calcium imaging study. *J. Neurophysiol.*, **87**, 1106–1117.
- Sadek, M.M., Hansson, B.S., Rospars, J.P. & Anton, S. (2002) Glomerular representation of plant volatiles and sex pheromone components in the antennal lobe of the female *Spodoptera littoralis*. *J. Exp. Biol.*, **205**, 1363–1376.
- Spors, H. & Grinvald, A. (2002) Spatio-temporal dynamics of odor representations in the mammalian olfactory bulb. *Neuron*, **34**, 301–315.
- Stopfer, M., Bhagavan, S., Smith, B.H. & Laurent, G. (1997) Impaired odour discrimination on desynchronization of odour-encoding neural assemblies. *Nature*, **390**, 70–74.
- Stopfer, M., Jayaraman, V. & Laurent, G. (2003) Intensity versus identity coding in an olfactory system. *Neuron*, **39**, 991–1004.
- Tolbert, L.P. & Hildebrand, J.G. (1981) Organization and synaptic ultrastructure of glomeruli in the antennal lobes of the moth *Manduca sexta*: a study using thin sections and freeze-structure. *Phil. Trans. R. Soc. Lond. B*, **213**, 279–301.
- Uchida, N. & Mainen, Z.F. (2003) Speed and accuracy of olfactory discrimination in the rat. *Nat. Neurosci.*, **6**, 1224–1229.
- Vosshall, L.B., Wong, A.M. & Axel, R. (2000) An olfactory sensory map in the fly brain. *Cell*, **102**, 147–159.
- Waldrop, B.R., Christensen, T.A. & Hildebrand, J.G. (1987) GABA-mediated synaptic inhibition of projection neurons in the antennal lobes of the sphinx moth, *Manduca sexta*. *J. Comp. Physiol. A*, **161**, 23–32.
- Wehr, M. & Laurent, G. (1996) Odour encoding by temporal sequences of firing in oscillating neural assemblies. *Nature*, **384**, 162–166.
- Wise, P.M. & Cain, W.S. (2000) Latency and accuracy of discriminations of odor quality between binary mixtures and their components. *Chem. Senses*, **25**, 247–265.